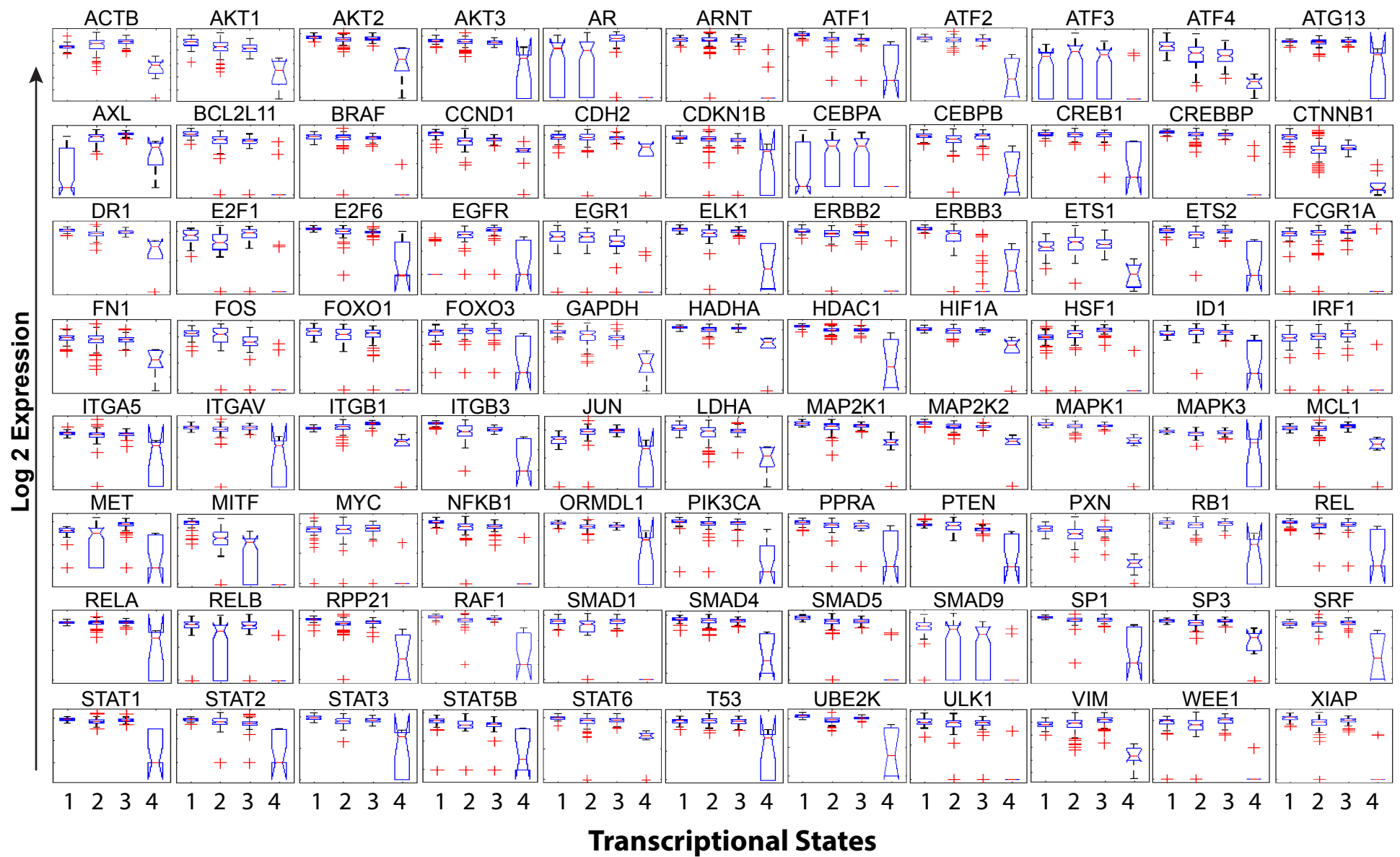
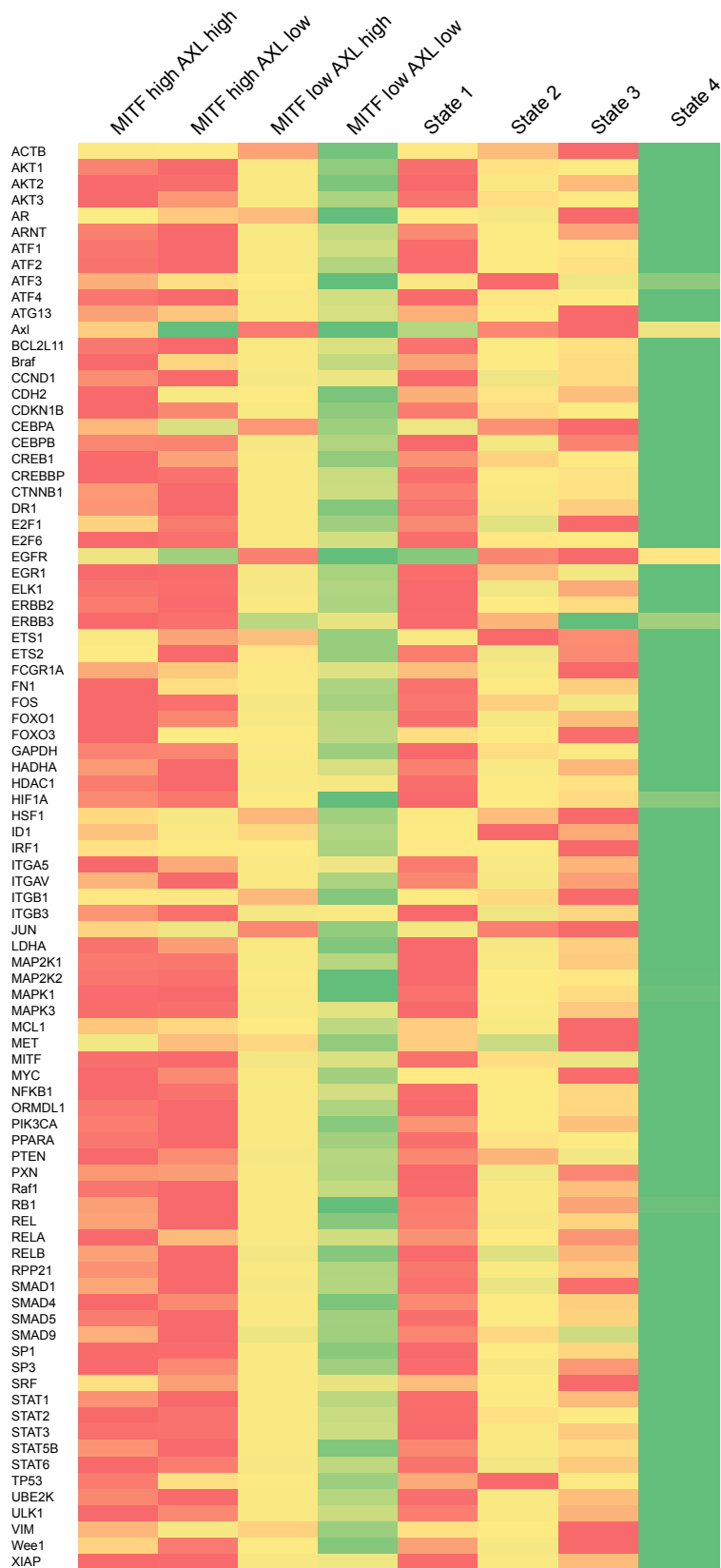


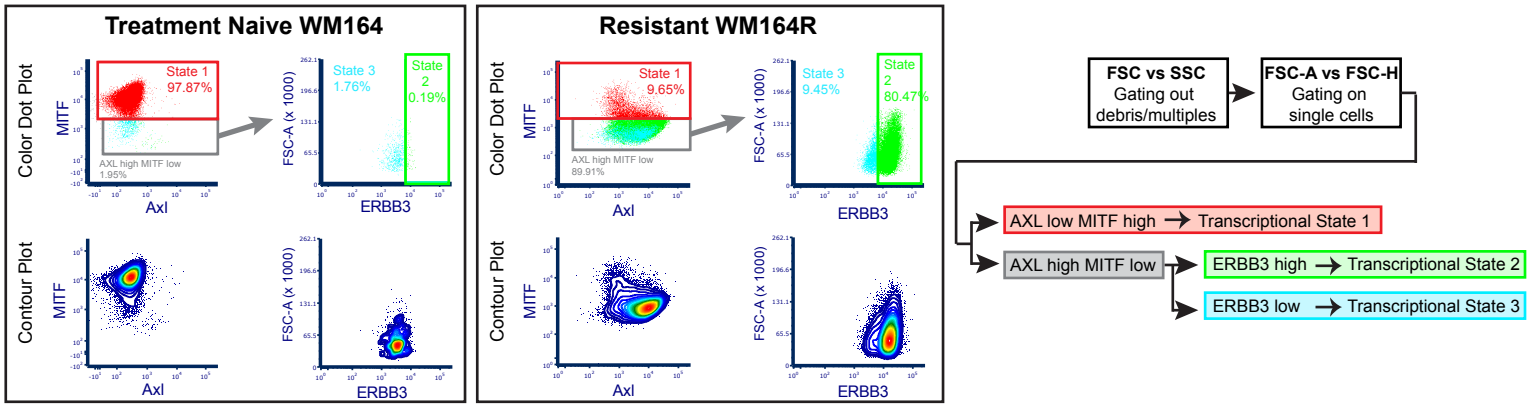
Supplemental Figure 1. Identifying the number of transcriptional states using SinCHET. SinCHet provides Shannon Profile (SP) for each cell line by evaluating the heterogeneity using Shannon index at different heights along the dendrogram (Figure 1B). PSD, the profile of the differences of Shannon index is then calculated along the same X-axis as SP, and is used to characterize the heterogeneity differences between two cell lines. **A.** The change points of the profile of Shannon differences (PSD) were detected by multivariate adaptive regression splines (MARS) model in each pair comparison. **B.** Shannon profiles of two conditions with D statistics and its p values estimated by 1000 permutation in each pair comparison. **C.** Heatmap of gene expression data of 88 genes (y-axis) for individual cells (x-axis) of treatment-naive WM164 and 1205Lu and their drug-resistant (R) counterparts. Color-coding under the dendrogram depicts the transcriptional state and the cell line each cell belongs to. The first change point determined by MARS is chosen as the optimum analysis point to maximize the number of cells in each state and to maximize the statistical power of comparison among the transcriptional states. This change point is used to determine the landscape of the transcriptional states present in each cell line (Figure 1F).



Supplemental Figure 2. Unique transcriptional profiles observed in four transcriptional states. Violin plots showing expression of each of the 88 mRNAs clustered by transcriptional state (bars representing state #1 to state #4 from left to right). Note higher Axl and c-JUN in states #2 and #3, Cyclin D1 (CCND1), MITF in state #1, ERBB3 in states #1 and #2

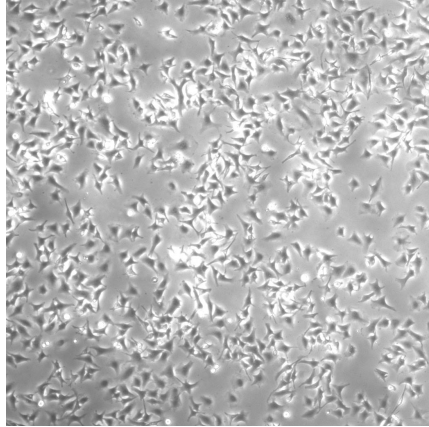


Supplemental Figure 3. Comparison of MITF high/low and AXL high/low subpopulations with the 4 transcriptional states identified by SinCHet. Heatmap of gene expression profiles among subpopulations of cells clustered by MITF high/low and AXL high/low and transcriptional state 1-4 identified by SinCHet. Data show that MITF high/ AXL low and MITF low/AXL high signatures are not binary states and that a range of intermediary phenotypes exist.

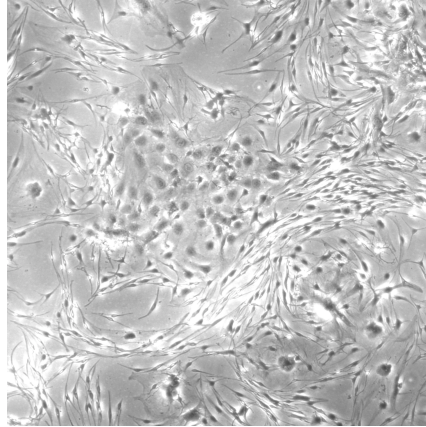


Supplemental Figure 4. Flow cytometry can be used to distinguish the three major transcriptional states based upon expression of MITF/AxL/ERBB3. Figure shows flow cytometry gating for AxL, MITF and ERBB3 for the treatment-naïve WM164 and drug-resistant WM164R cells.

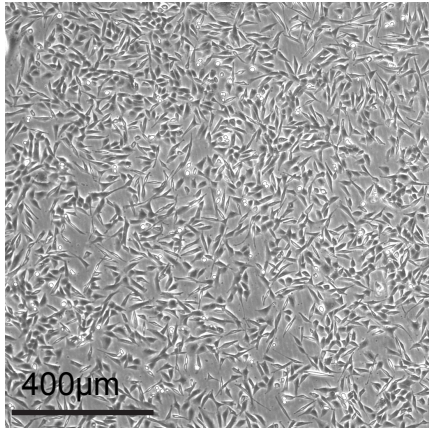
WM164



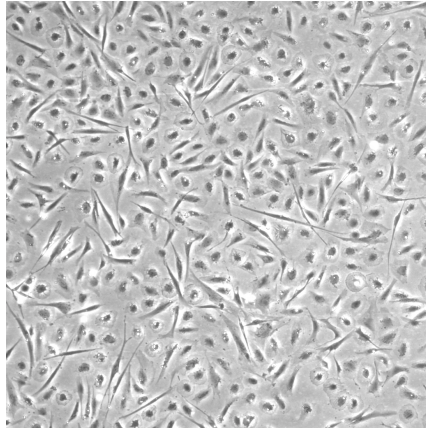
WM164R



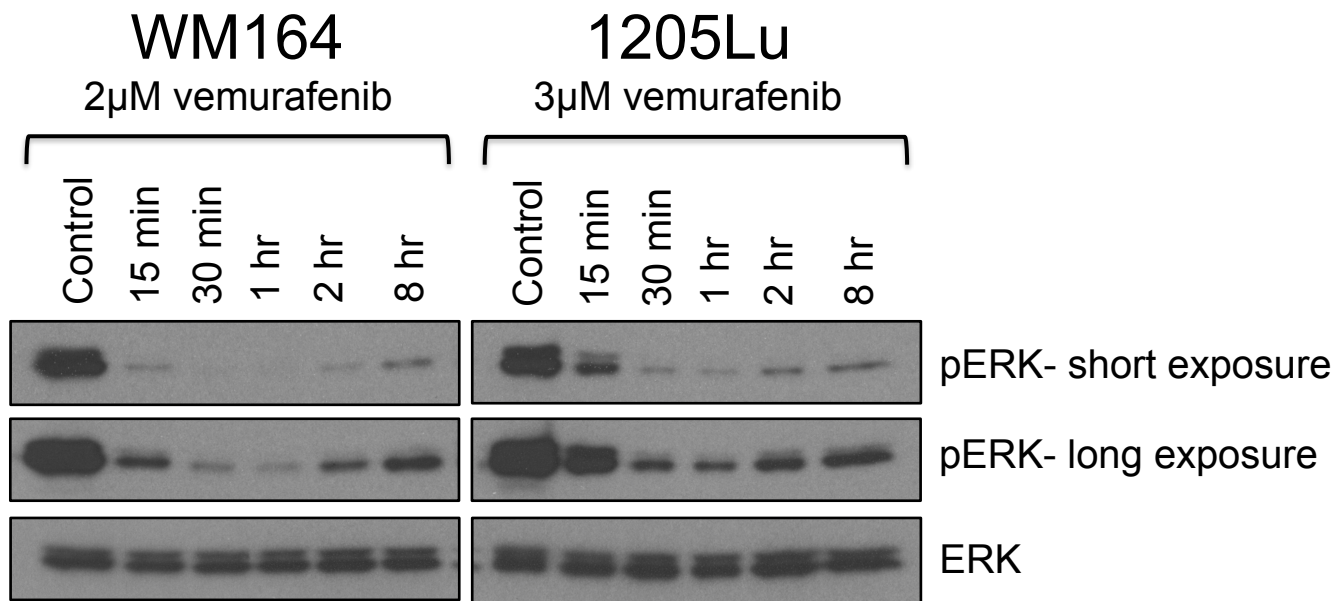
1205Lu



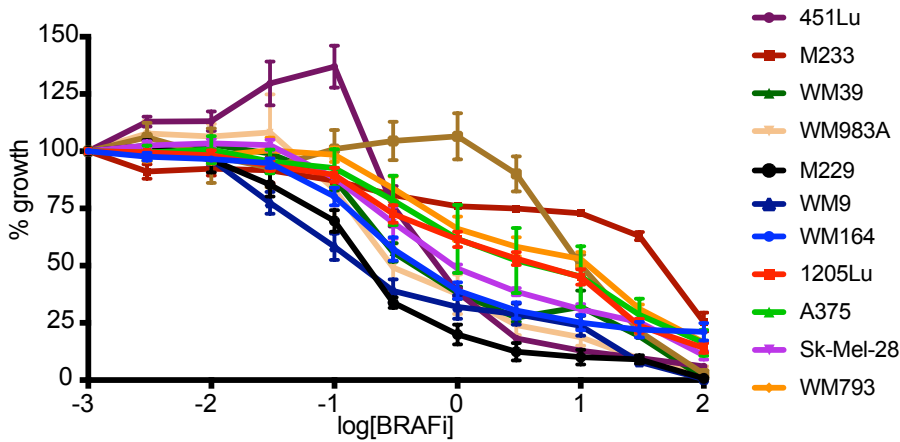
1205LuR



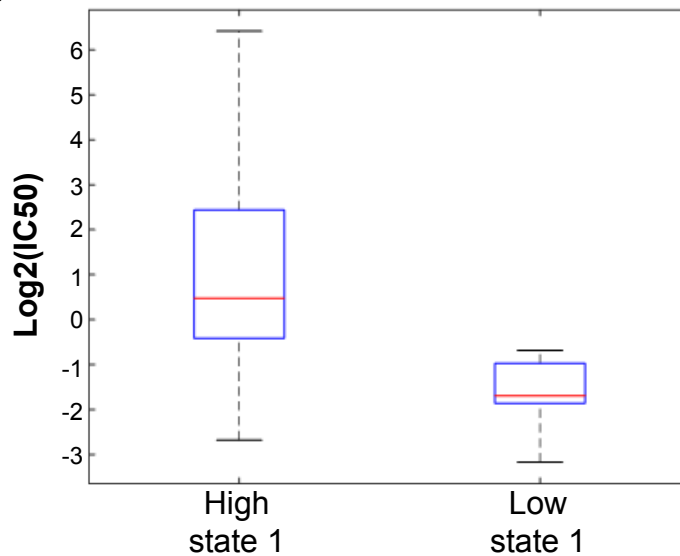
Supplemental Figure 5. Heterogeneity in cell morphologies. The changes in transcriptional diversity observed in Figure 1 were also mirrored by changes in the diversity of cell morphologies. Brightfield microscopy taken using a 10x magnification lens.



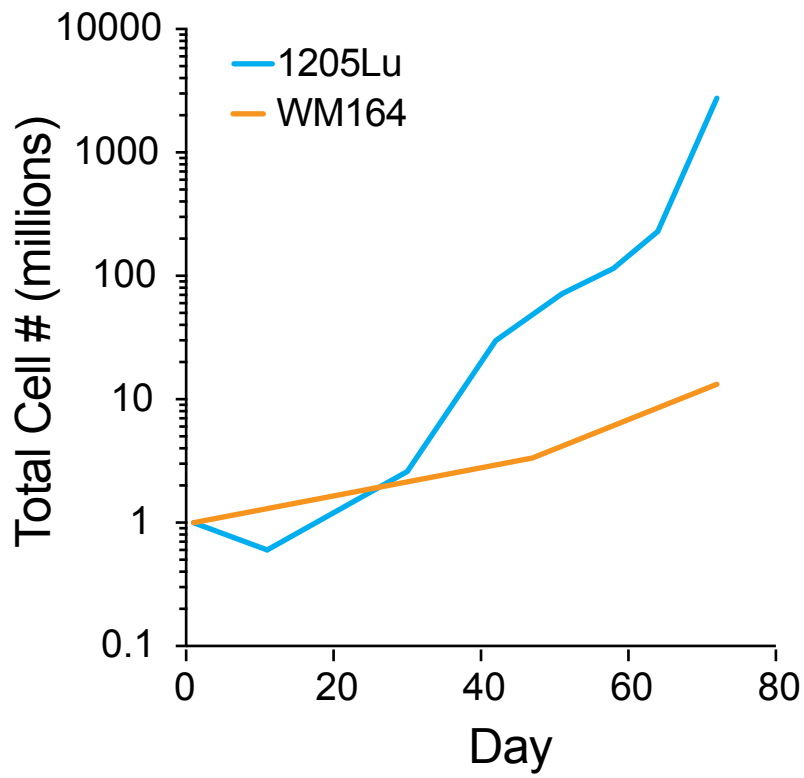
Supplemental Figure 6. Equivalent ERK inhibition between cell lines. Western blot analysis shows equivalent levels of ERK inhibition over an 8-hour time course with vemurafenib.

A**MTT Assay**

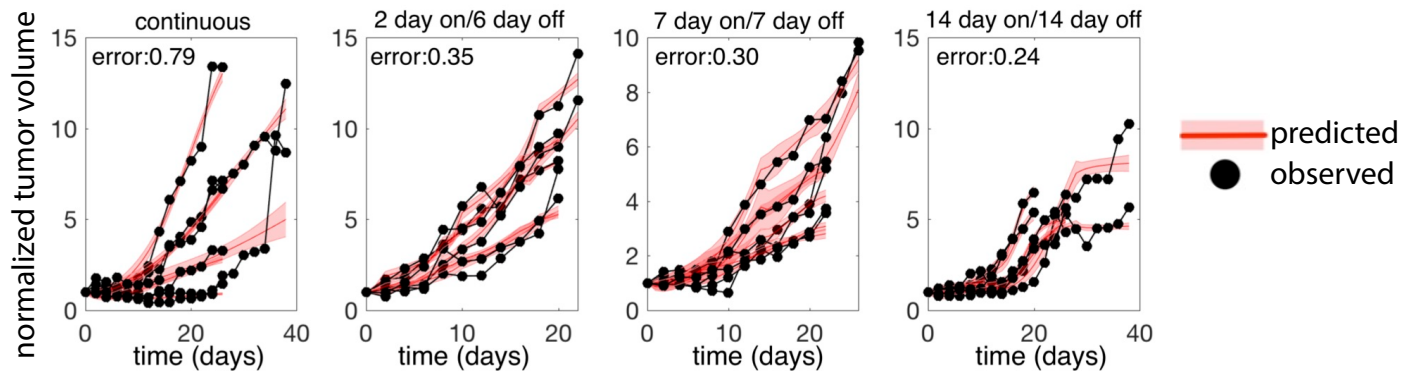
Cell Line	IC50	95% CI
WM9	0.111	0.06553 to 0.1908
M229	0.156	0.1192 to 0.2044
WM164	0.275	0.207 to 0.3666
WM983A	0.284	0.1577 to 0.5295
WM39	0.337	0.2195 to 0.5235
Sk-Mel-28	0.509	0.3582 to 0.7283
451Lu	0.623	0.3826 to 1.03
A375	1.262	0.4213 to 4.081
1205Lu	1.391	0.8765 to 2.223
WM793	2.158	1.048 to 4.698
M233	85.310	27.79 to 2070

B

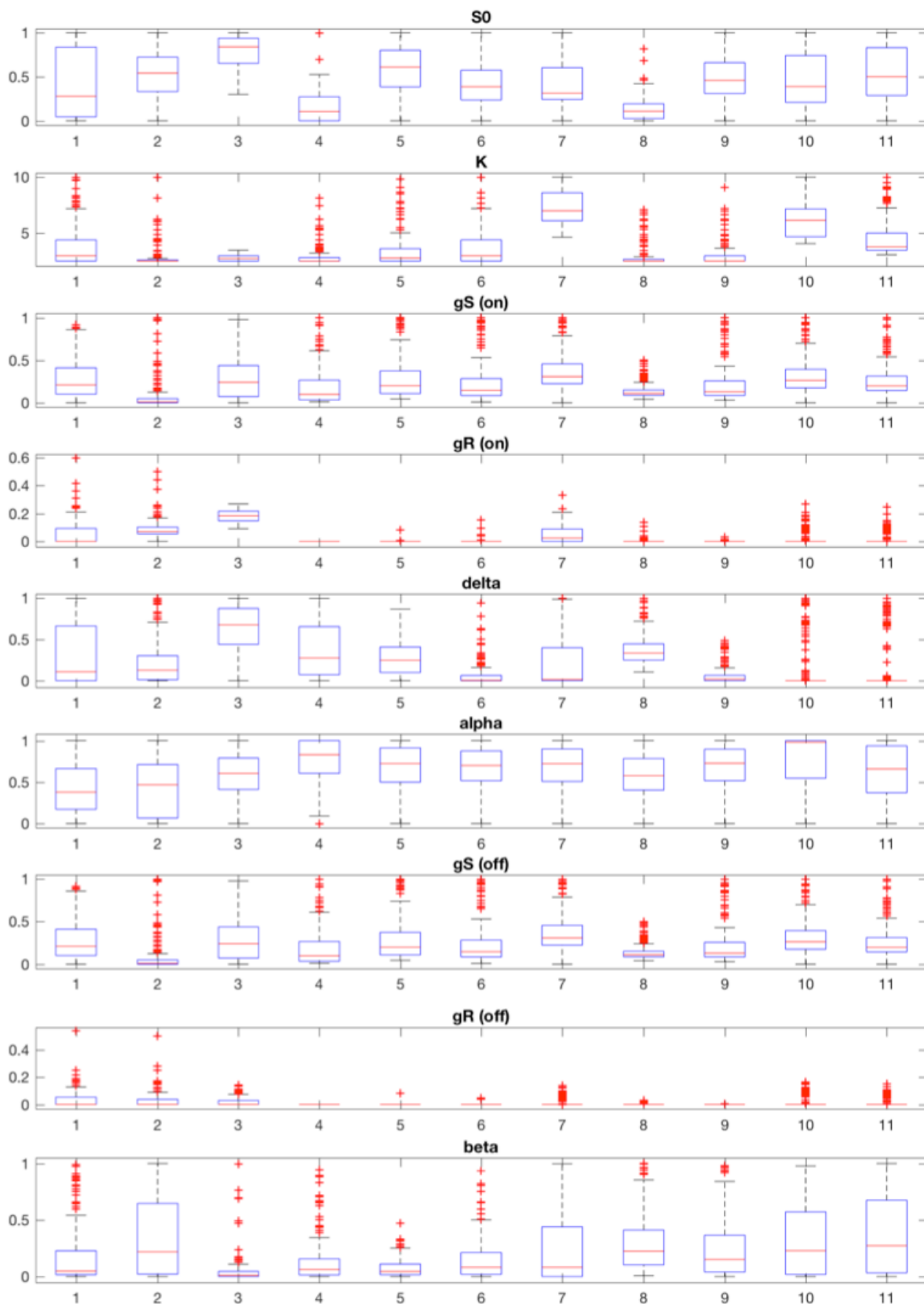
Supplemental Figure 7. The sensitivity of a melanoma cell line panel to the BRAF inhibitor vemurafenib is associated with proportion of cells in transcriptional state 1. A. MTT-based growth inhibition analysis shows differences in vemurafenib sensitivities to increasing doses of the drug among 11 human melanoma cell lines (left panel). Error bars represent standard error of the mean. IC₅₀ values are calculated using non-linear regression analysis of log(inhibitor) vs response (right panel). **B.** Comparison of the log₂(IC₅₀) between the cell lines with high (greater than 50%) and low (less than 50%) proportion of cellular state 1. A two-sample t-test ($t = -2.02$, $p = 0.07$).



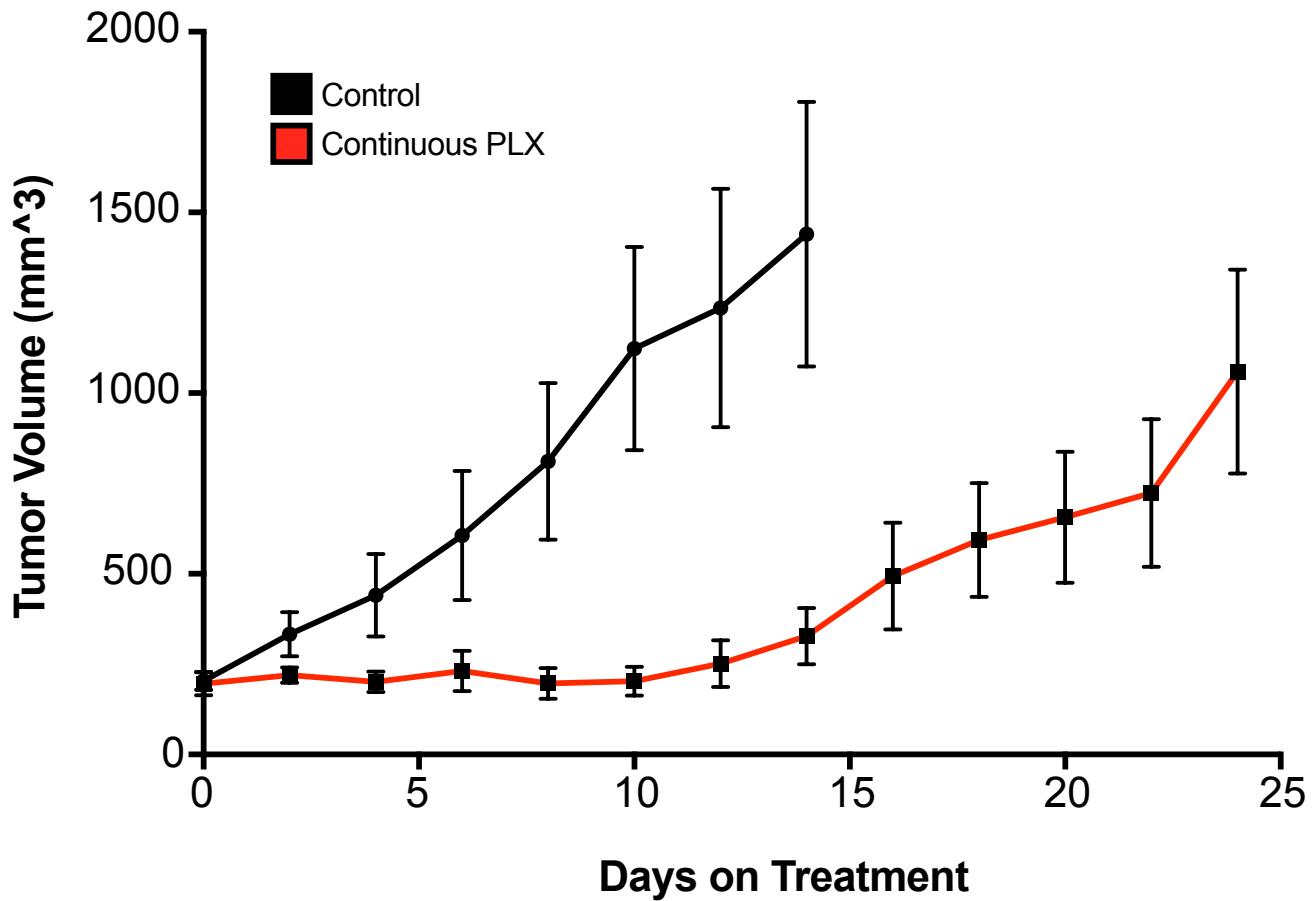
Supplemental Figure 8. Faster onset of drug resistance in cell line lacking state 1. Comparison of cell growth of treatment-naive melanoma cell lines modeled from empirically measured growth rates over chronic treatment time (vemurafenib; 3 μ M for 1205Lu, 2 μ M for WM164).



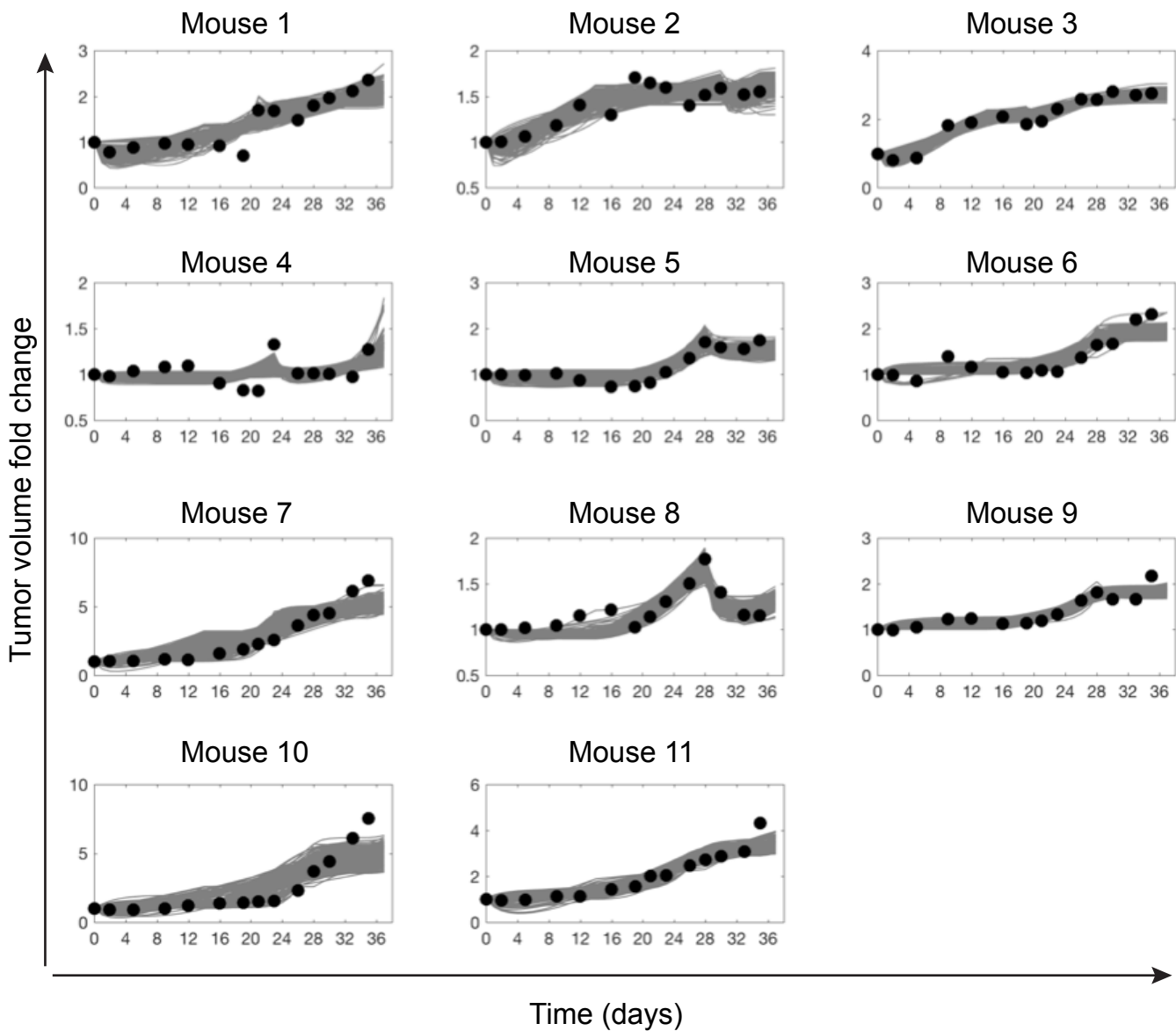
Supplemental Figure 9. Mathematical model calibration. To predict an effective intermittent inhibitor therapy schedule, the model was calibrated to xenograft tumour growth dynamics. WM164 cell line was implanted as subcutaneous xenografts at two million cells per injection and allowed to establish over several days. Mice were treated with PLX4720-formulated diet using continuous, 2-day on/6-day off, 7-day on/7-day off and 14-day on/14-day off schedules. These estimated parameters were later used as initial ranges for parameterizing the mathematical model to determine the individual mouse-specific treatment schedules on the adaptive treatment arm (Figure 5). Black dot: Observed tumor volume fold change ($V(t)/V(t=0)$, V : volume, t : time), red line: average model prediction.



Supplemental Figure 10. Distribution of estimated parameters for 11 different mice. The x-axis represents the mouse ID number, S0: initial sensitive cell proportion, K: carrying capacity, gS (on): growth rate of sensitive cell during treatment on, gR (on): growth rate of resistant cell during treatment on, delta: death rate of sensitive cells due to treatment, alpha: S→R transition rate, gS (off): growth rate of sensitive cell during treatment off, gR (off): growth rate of resistant cell during treatment off, beta: R→S, transition rate.



Supplemental Figure 11. BRAF inhibitor-formulated mouse chow inhibits melanoma xenograft growth. Female SHO mice (Charles River) were subcutaneously injected with WM164 cell line (2.5×10^6 cells per mouse, 6 mice per treatment group). Tumors were allowed to grow to ~ 100 mm³, then mice were fed either D10001 control chow or AIN-76A 417 mg kg⁻¹ PLX4720-formulated chow (Research Diets, New Brunswick, NJ). Average tumor volumes of xenografted WM164 cell line are shown based on the modified ellipsoid formula (tumor volume = $\frac{1}{2} \times L \times W^2$).



Supplementary Figure 12. Mathematical model fits to observed tumor measurements for each mouse. Model predictions of tumor volume fold change ($V(t)/V(t=0)$, V : volume, t : time) from day 0 to day 37 (gray lines, 200 predicted model fits per mouse) fit to the measured tumor volumes (black dots). Tumor volume fold change ($V(t)/V(t=0)$, V : volume, t : time).